Proceedings of the Combustion Institute 40 (2024) 105581

Contents lists available at ScienceDirect

Proceedings of the Combustion Institute

journal homepage: www.elsevier.com/locate/proci

The importance of Soret effect, preferential diffusion, and conjugate heat transfer for flashback limits of hydrogen-fueled perforated burners

Filippo Fruzza [a], Hongchao Chu [b], Rachele Lamioni [a,*], Temistocle Grenga [c], Chiara Galletti [a], Heinz Pitsch [b]

[a] Dipartimento di Ingegneria Civile e Industriale, Università di Pisa, 56122 Pisa, Italy
[b] Institute for Combustion Technology, RWTH Aachen University, Aachen 52056, Germany
[c] Faculty of Engineering and Physical Sciences, University of Southampton, Southampton SO17 1BJ, UK

ARTICLE INFO

Keywords:
Flashback
Premixed hydrogen flame
Preferential diffusion
Soret effect
Perforated burner

ABSTRACT

Avoiding flashback is a primary challenge in the development of modern burners, which should be capable of substituting natural gas with hydrogen in domestic end-user devices. The heat exchange between the burner plate and the burned and unburned gases, as well as the effects of preferential diffusion, significantly impact the flashback of such burners fueled with hydrogen. For these effects, the design of the burner plate plays a pivotal role. In this study, three-dimensional simulations with detailed chemistry have been performed to investigate the effect of three competing physical mechanisms, namely, preheating of fresh gases, preferential diffusion, and Soret effect, which drive the flame flashback dependence on the holes/slits size. Two different geometries are considered: circular holes with varying diameters and slits with fixed lengths but different widths. Steady-state simulations with decreasing inlet velocities are employed to estimate the critical inlet velocity for flashback. Conjugate heat transfer (CHT) is considered for the heat exchange between the burner plate and the gases. For circular holes, the enclosed geometry promotes more effective heat transfer, leading to a higher influence of preheating effects for small diameters. This results in a non-monotonic dependence on hole size, with a non-trivial optimum diameter to avoid flashback. This behavior is specific to circular holes and differs from that observed in previously studied infinitely long slits, where a linear dependence on the slit width was found. Additionally, the individual influence of non-unity Lewis numbers and Soret diffusion is analyzed. Notably, the Soret effect, in combination with CHT, is found to instaurate a strong, non-linear, self-accelerating mechanism that has a leading-order effect on the flashback propensity of larger holes. This finding underscores the necessity of including both effects in numerical simulations for accurate estimations of the flashback limits in domestic burners.

1. Introduction

In the context of the massive incorporation of renewable resources, green hydrogen has emerged as a valid candidate to boost decarbonization in several sectors, including heating for residential and commercial buildings [1]. Current heating devices are mainly fueled with natural gas. They are equipped with flat or cylindrical burners that stabilize the flame on perforated plates, typically featuring patterns of circular holes and slits. The transition from natural gas to hydrogen presents significant challenges in burner design due to the high flame speed of hydrogen. Additionally, the impact of preferential diffusion and the Soret effect must be considered. The Soret effect, also known as thermal diffusion, is a process where species are transported under the influence of a temperature gradient: lighter species, such as H_2, exhibit negative coefficients, diffusing from cold to hot regions, whereas heavier species behave oppositely [2].

A critical challenge in this transition is to prevent the flashback of hydrogen flames, an undesirable phenomenon where the flame propagates upstream of the burner plate into a preheating region, posing significant safety risks. Flashback limits in domestic burners fueled with hydrogen and hydrogen/methane blends have been investigated both experimentally and numerically. On the experimental front, the burner temperature was identified as a crucial factor influencing flashback [3,4], and autoignition was explored as an alternative flashback initiation mechanism [5]. On the numerical front, primarily two-dimensional (2D) configurations were employed to simulate flashback in perforated burners [6–11]. Due to the importance of the burner temperature for

* Corresponding author.
E-mail address: rachele.lamioni@unipi.it (R. Lamioni).

https://doi.org/10.1016/j.proci.2024.105581
Received 4 December 2023; Accepted 2 July 2024
Available online 23 July 2024

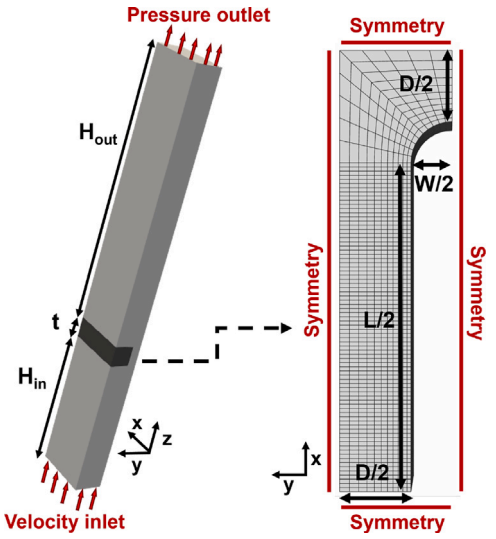

Fig. 1. Left panel: computational domain (fluid zone in light gray, solid zone in dark gray). Right panel: slit geometry. Boundary conditions are indicated in red.

the flashback propensity, numerical models including the conjugate heat transfer were found to be necessary for a correct estimation of the flashback limits [6,7,9]. Additionally, non-unity Lewis numbers and Soret diffusion were found to play a key role for the stabilization of premixed flames in bluff-body configurations by Vance et al. [12,13]. In recent works by Fruzza et al. [9,11] and Flores-Montoya et al. [10], two distinct flashback regimes were observed for CH_4-H_2-air mixtures when varying the H_2 content: a bulk symmetric flashback and an asymmetric flashback.

In a recent study, Fruzza et al. [14] addressed the limitations of 2D simulations by comparing them to 3D simulations. The findings revealed significant differences between 2D and 3D results for practical slits, underscoring the intrinsic three-dimensional nature of flashback dynamics.

A crucial geometrical parameter influencing flashback in the design of perforated burners is the diameter of the holes or the width of the slits. This parameter has a substantial impact on the heat exchange between the burner plate and the gases, as well as on the effects of preferential diffusion, which plays a significant role in flashback [7,11]. In this study, we employ detailed numerical simulations to examine the influences of preheating, preferential diffusion, and the Soret effect in determining the dependence of flashback limits for H_2-air flames on the hole/slit size. Two configurations are investigated: circular holes with varying diameters and slits with fixed length and varying widths. To assess the effects of the hole/slit size on preferential diffusion caused by both the non-unity Lewis number and the Soret effect, simulations are also conducted with the unity-Lewis-number assumption and neglecting Soret diffusion. Specifically, the Soret effect is identified as playing a leading-order role in determining the dependence on the hole size, due to a non-linear feedback mechanism that narrows the flashback limits for larger holes.

2. Configuration and numerical methods

3D configurations representing arrays of holes or slits of different shapes and sizes are considered, emulating a portion of a real burner plate typically used in domestic condensing boilers. The computational domain is shown in Fig. 1, where the slit geometry is shown in the right panel. The slit width is denoted by W, while the distance between two adjacent slits is denoted by D. The distance between the centers of the round far ends of the slit is represented by L, so that $L = 0\,\text{mm}$ corresponds to a circular hole of diameter W. The burner plate thickness is $t = 0.6\,\text{mm}$ for all cases. Two different shapes are investigated: circular holes with varying diameters, for which W is varied within the range $W \in [0.4\,\text{mm}–0.8\,\text{mm}]$, and slits with fixed length $L = 2\,\text{mm}$ and width W varied in the same range. The porosity of the burner is defined as $\psi = A_{\text{slit}}/A_{\text{tot}}$, where A_{slit} is the perforated area and A_{tot} is the sum of the plate and the perforated areas. For all the investigated geometries, the porosity is kept fixed at $\psi = 0.2$ by adjusting D when varying W. Maintaining a constant porosity is crucial as it allows the direct correlation of the flashback velocity to a specific power input to the burner covered with the simulated slit. Due to the symmetries of the problem, the computational domain can be reduced to a quarter of the entire hole/slit. Symmetry boundary conditions are imposed on the external edges of the domain, to consider the interaction with the adjacent holes/slits. The fluid domain extends enough both downstream ($H_{\text{out}} = 8\,\text{mm}$) and upstream ($H_{\text{in}} = 4\,\text{mm}$) of the solid. We use H_2-air mixtures at different equivalence ratios ϕ. Uniform velocity and uniform temperature of $T_u = 300\,\text{K}$ are set at the inlet, and a pressure of $p = 1\,\text{atm}$ is imposed at the outlet. At the fluid–solid interface, a no-slip boundary condition is imposed for the velocity, and zero-mass flux is imposed for the species. No thermal boundary conditions are needed at the fluid–solid interface since the heat fluxes are computed directly as described below.

For the fluid, transport equations of mass, momentum, energy, and mass fractions of chemical species are solved. The gas phase is modeled as an ideal gas. Inside the solid domain, the energy equation is solved. The burner plate is modeled as a solid with properties representative of practical stainless steel commonly used in burners, with density $\rho_s = 7719\,\text{kg m}^{-3}$, specific heat $c_{p,s} = 461.3\,\text{J kg}^{-1}\,\text{K}^{-1}$, and thermal conductivity $k_s = 22.54\,\text{W m}^{-1}\,\text{K}^{-1}$. The equations are solved on a structured grid, with characteristic cell size in the reaction region of $\Delta x = 25\,\mu\text{m} \simeq \delta_F/13$, where δ_F is the 1D unstretched thermal flame thickness computed for $\phi = 1.0$. The mesh is slightly stretched in both the x and y directions toward the domain boundaries and in the z direction toward the inlet and outlet, far from the reaction zone. Detailed chemistry for hydrogen-air mixtures is employed, utilizing a reduced version of the Kee-58 skeletal mechanism [15] including 9 chemical species and 19 reactions. Full multicomponent diffusion is modeled using generalized Fick's law coefficients derived from the Maxwell–Stefan equations [16–18]. Soret diffusion is modeled using the empirically-based composition-dependent expression provided by Kuo [16,19] as

$$D_{T,i} = -\alpha T^{\beta} \frac{\sum_j M_j^{\gamma} X_j}{\sum_j M_j^{\eta} X_j} \left(\frac{M_i^{\gamma} X_i}{\sum_j M_j^{\gamma} X_j} - Y_i \right), \tag{1}$$

where $\alpha = 2.59 \times 10^{-7}$, $\beta = 0.659$, $\gamma = 0.511$, and $\eta = 0.489$ are empirical constants, while M_i, X_i, and Y_i are the molar mass, molar fraction, and mass fraction of the species i, respectively. The gray Discrete Ordinates (DO) method [20] is employed to model radiation, assuming the emissivity of the fluid–solid interface to be 0.85. The conjugate heat transfer between the fluid and the solid zones is modeled using Fourier's Law to compute the heat flux through the fluid–solid interface [16]. It should be noted that no turbulence model is required, as all simulations exhibit fully laminar flow, which is typical for domestic burners.

3. Solution methodology

We performed steady-state simulations using the ANSYS-Fluent 22.1 pressure-based coupled algorithm [16] and a second-order upwind scheme for spatial discretization. To determine the critical inlet velocity for flashback, simulations for each investigated condition start with a relatively high inlet velocity, leading to a stable flame. This inlet velocity is progressively decreased until the steady-state solver can no longer find a stable flame solution, indicating that the critical inlet velocity for flashback has been reached. To estimate accurately the flashback inlet velocity, the minimum decrement of the inlet velocity is specified as $\Delta V_{\text{in}} = 0.01\,\text{m/s}$. The cold-flow bulk velocity at the slit entry is defined

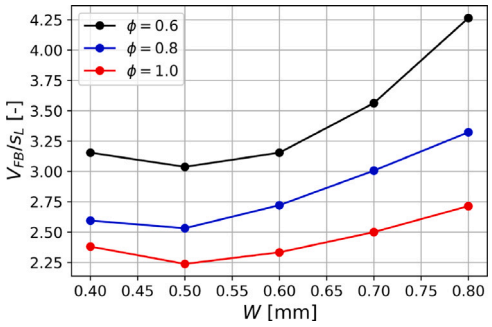

Fig. 2. Normalized flashback velocity as a function of hole diameter for $\phi = 0.6$, 0.8, and 1.0. (For interpretation of the references to color in this figure legend, the reader is referred to the web version of this article.)

considering the porosity of the burner as $V_S = A_{tot}/A_{slit}\ V_{in} = 1/\psi\ V_{in}$. Following Vance et al. [7], the flashback velocity V_{FB} is defined as

$$V_{FB} = V_S|_{FB} = \frac{1}{\psi} V_{in}|_{FB}. \tag{2}$$

This methodology has been validated in previous studies using detailed transient simulations [14]. We point out that no thermo-diffusive instabilities were observed for the investigated cases.

4. Results and discussion

4.1. Circular holes

This section discusses the effects of the diameter of circular holes on the flashback velocity for three equivalence ratios of $\phi = 0.6$, 0.8, and 1.0. Flashback velocities are computed for varying diameters in the range $W \in [0.4\,\text{mm}–0.8\,\text{mm}]$. The results are shown in Fig. 2, where V_{FB} is normalized with the unstretched laminar flame speed of the corresponding mixtures. As expected, V_{FB}/s_L is higher for leaner mixtures due to the impact of preferential diffusion, which is consistent with previous findings [7,11]. All curves exhibit similar trends, featuring a weak dependence of the flashback velocity on the hole diameter from $W = 0.4\,\text{mm}$ to $W = 0.5\,\text{mm}$, succeeded by a nonlinear increase for $W > 0.5\,\text{mm}$. This behavior is unique to circular holes, contrasting with infinitely long slits previously examined in the literature that exhibit a linear dependence on the slit width [7]. Further, the slope of the curve in the region with larger diameters increases as the equivalence ratio decreases. This trend can be explained by the relative importance of three effects: preheating of the unburnt mixture, preferential diffusion, and the Soret effect. The dominance of one effect or the other is found to lead to the occurrence of two distinct flashback mechanisms, which clarifies the non-monotonic dependence of V_{FB}/s_L on the slit width and will be discussed in more detail next.

In Fig. 3, we show the distribution of temperature, normalized equivalence ratio, and H_2 consumption rate for the last stable flame before flashback with $W = 0.4\,\text{mm}$ and $W = 0.8\,\text{mm}$, highlighting the two flashback mechanisms. The local equivalence ratio φ is defined using the Bilger formula [15] and normalized with the equivalence ratio of the inlet mixture $\phi_{in} = 0.6$. The molecular H_2 consumption rate ω_{H_2} is normalized with the maximum H_2 consumption rate obtained for the corresponding 1D flame $\max(\omega_{H_2,1D})$. To visualize the flame front, progress variable iso-contours are included. The progress variable is defined as $C = 1 - Y_{H_2}/Y_{H_2,u}$, where Y_{H_2} denotes the H_2 mass fraction, and $Y_{H_2,u}$ represents its value in the unburnt mixture.

For $W = 0.4\,\text{mm}$, the flame is very close to the hole exit. No significant enrichment is observed in this region, resulting in a relatively uniform H_2 consumption rate along the flame front for a given C. This is due to the less significant role of the Soret effect and preferential diffusion compared to the case of $W = 0.8\,\text{mm}$. The relationship between the geometrical dimensions and the impact of the different physical mechanisms will be explored in greater detail next. Due to the small size of the channel, with the thermal boundary layer thickness being comparable with the radius of the hole, the mixture temperature is approximately uniform when reaching the flame zone, with $T \simeq 900\,\text{K}$ at $C = 0.3$. The preheating of fresh gases is due to the heating of the flow when passing through the hot hole: at steady-state, the heat lost by the flame to the burner at the top of the plate is provided back to the flow on the bottom and the inner surface of the plate (net of losses through radiation), causing the gases to be preheated. This mechanism is illustrated in Fig. 3(a), where the heat flux is indicated as $\dot{Q}$. When the inlet velocity is decreased, the flame finds a new stable position, closer to the burner plate, further increasing the solid temperature and the preheating of the mixture. The preheating of the fresh gases has two competing effects on the stabilization of the flame. On the one hand, the flow velocity increases linearly with temperature due to the decreased density. Since flashback occurs when the flame speed is higher than the flow velocity, this mechanism would suppress flashback. On the other hand, the flame speed increases with the unburnt mixture temperature. However, s_L increases more than linearly with the mixture temperature [21], and thus faster than the flow velocity. When reducing the inlet velocity, the preheating is progressively intensified until a critical inlet velocity and a critical mixture temperature are reached. At this point, the flame speed surpasses the bulk velocity, causing the flame to propagate into the hole.

For the case with $W = 0.8\,\text{mm}$, the main driver for flashback is preferential diffusion due to the less-than-unity Lewis number of the mixture and the Soret effect. For mixtures with effective Lewis numbers smaller than unity, preferential diffusion leads to a leaner mixture at the negatively curved tip of the flame (zone A in Fig. 3(b)), and thus a subsequent enrichment in the flame base region (zone B) [22]. Additionally, the hole is sufficiently wide to sustain a cold flow at its center, resulting in a non-uniform unburnt mixture temperature at the hole exit, varying from $T \simeq 400\,\text{K}$ to $T \simeq 1000\,\text{K}$ along the $C = 0.3$ iso-line. Soret diffusion, induced by strong temperature gradients, causes the light H_2 species to diffuse toward hotter regions, leading to the enrichment of the mixture upstream of the burner and close to the hot burner plate (zone C). This increases the heat release and the temperature gradients in this region, thereby promoting the Soret effect. This is similar to the self-supporting mechanism discussed for a bluff-body configuration by Vance et al. [13]. Both of these effects result in an enrichment of the mixture in the flame base region near the burner plate, with a peak of $\varphi/\phi_{in} \simeq 1.4$. Consequently, the hydrogen consumption rate and the flame speed increase at the flame base, and flashback is initiated in the critical region close to the wall where the gas velocity is small.

The shape of the curve in Fig. 2 is determined by the relative importance of preheating and preferential diffusion. However, a detailed quantification of the individual contributions of preheating and preferential diffusion and a comprehensive understanding of their interactions as the hole diameter varies cannot be readily extracted from the above analysis. Moreover, the specific contributions of non-unity Lewis numbers and Soret diffusion and their influence on the flashback velocity as the hole diameter varies are not yet clear. This investigation is crucial to determine the necessity of including these two effects in numerical simulations for an accurate estimation of the flashback limits. To address this, flashback velocities are computed by independently switching off these two effects while varying the diameter in the same range as above for the case $\phi = 0.6$. To eliminate the effect of non-unity Lewis numbers, diffusion coefficients are computed by assigning unity Lewis numbers for all species instead of employing the full multicomponent diffusion model. Soret diffusion is neglected by eliminating the temperature gradient-dependent term in the species equations. This approach results in four cases: two for each effect being neglected individually and two where either both effects are omitted or considered. The laminar flame speeds and flame thicknesses used

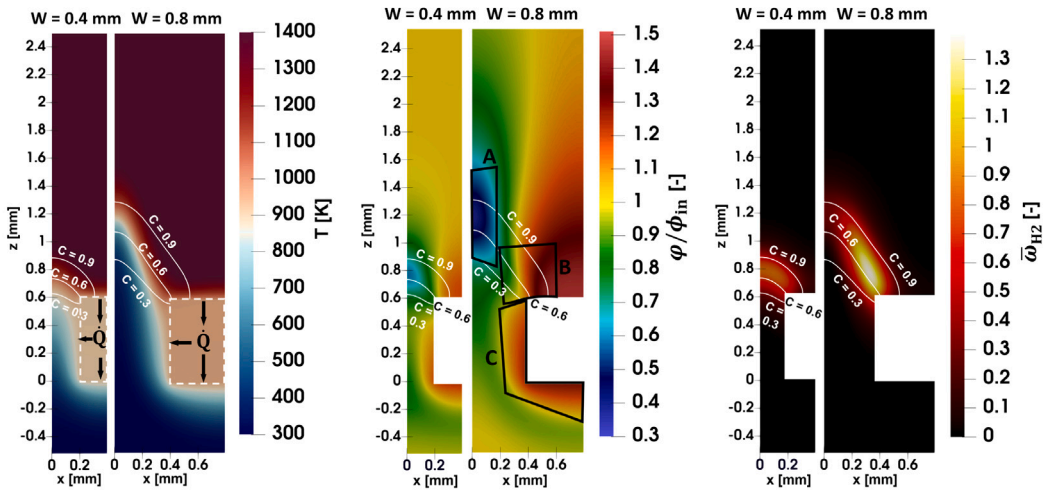

Fig. 3. Visualization of temperature (a), normalized local equivalence ratio (b), and normalized H_2 consumption rate (c) profiles for two circular holes with $W = 0.4\,\text{mm}$ and $W = 0.8\,\text{mm}$ at the flashback limit for the case $\phi = 0.6$. Progress variable iso-contours are plotted in white. The solid part is represented by a dashed line.

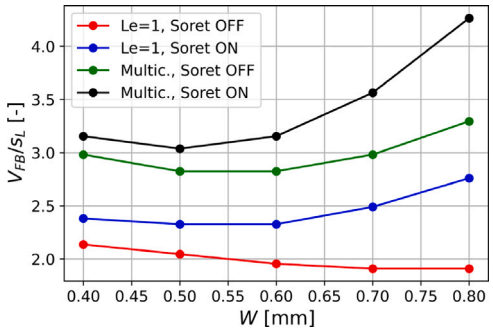

Fig. 4. Normalized flashback velocity as a function of hole diameter for the four investigated cases. For each case, V_{FB} is normalized with the corresponding s_L. (For interpretation of the references to color in this figure legend, the reader is referred to the web version of this article.)

Table 1
Averaged burner plate temperatures and heat fluxes at the top surface of the plate for $V_S = 4.00\,\text{m/s}$.

W [mm]	Case	T_B [K]	$\dot{q}$ [W/mm^2]
0.4	$Le = 1$, Soret OFF	716	0.449
	$Le = 1$, Soret ON	759	0.516
	Multic., Soret OFF	849	0.627
	Multic., Soret ON	843	0.625
0.8	$Le = 1$, Soret OFF	738	0.362
	$Le = 1$, Soret ON	848	0.612
	Multic., Soret OFF	917	0.540
	Multic., Soret ON	940	0.580

for the normalization of these three cases are also obtained using the corresponding diffusion models. The normalized flashback velocities are shown in Fig. 4 as functions of the hole diameters. It is interesting to note that, when the effects of Soret diffusion and non-unity Lewis numbers are eliminated, the flashback velocity exhibits a monotonic negative dependence on the hole diameter. In contrast, when these effects are present (individually or together), a non-monotonic dependence is observed, with V_{FB} decreasing with W for $W < 0.5\,\text{mm}$, and increasing for larger diameters.

To better understand the mechanisms driving flashback for small and large diameters in the four different cases shown in Fig. 4, 2D fields of normalized H_2 consumption rate and normalized local equivalence ratio are shown in Figs. 5(a) and (b) for the extreme diameters $W = 0.4\,\text{mm}$ and $W = 0.8\,\text{mm}$, respectively. For a consistent comparison, the results are shown for a fixed slit velocity $V_S = 4.00\,\text{m/s}$, which do not necessarily correspond to the last stable flames before flashback. Temperature iso-lines are included in the visualizations of $\bar{\omega}_{H_2}$, and progress variable iso-lines are included in the visualizations of the local equivalence ratio. The local equivalence ratio for the case "$Le = 1$ and Soret OFF" is not shown since no preferential diffusion is present and the equivalence ratio is uniform. In Fig. 6, we also present the variation of the displacement speed, s_D, along the flame front for all cases. The displacement speed is defined as $s_D = \rho/\rho_u \boldsymbol{v} \cdot \boldsymbol{n}$, where ρ is the density, ρ_u is the density of the fresh mixture, $\boldsymbol{v}$ is the flow velocity, and $\boldsymbol{n}$ is the unit vector normal to the temperature iso-surface corresponding to $T = 1200\,\text{K}$. Its value for each case is normalized with the corresponding laminar flame speed and plotted against the transversal coordinate x, scaled by the hole diameter W. To provide further support for the analysis, Table 1 reports the volume-averaged burner plate temperature, T_B, and the averaged heat flux lost by the flame at the top surface of the plate, $\dot{q}$, for the cases illustrated in Fig. 5.

When no preferential diffusion sources are present, the flame stabilization is driven solely by the unburnt gases preheating for all investigated diameters. A monotonic decrease in the flashback velocity with W can be observed in Fig. 4. This behavior can be attributed to more intense preheating for smaller diameters. As shown in Table 1, the more enclosed geometry of the case $W = 0.4\,\text{mm}$ leads to higher heat flux from the flame to the unburnt mixture with respect to $W = 0.8\,\text{mm}$. As a result, for $W = 0.4\,\text{mm}$, the unburnt mixture has a temperature of around 800 K when reaching the flame front region, while being approximately 600 K for $W = 0.8\,\text{mm}$. As discussed previously, a more intense preheating of the unburnt gases ultimately leads to higher flashback velocities, as the critical temperature at which the flame speed surpasses the bulk velocity is reached at higher inlet velocities. For this reason, the flashback velocity decreases as the hole diameter increases as shown in Fig. 4. Since no preferential diffusion effects are present, flashback is solely driven by preheating, which is more effective for smaller holes.

Enabling Soret diffusion does not result in significant changes for $W = 0.4\,\text{mm}$. Notable enrichment is primarily observed at the bottom and inner surface of the burner plate, where temperature gradients are higher. In contrast, the downstream part of the channel reaches a uniform gas temperature, resulting in lower temperature gradients

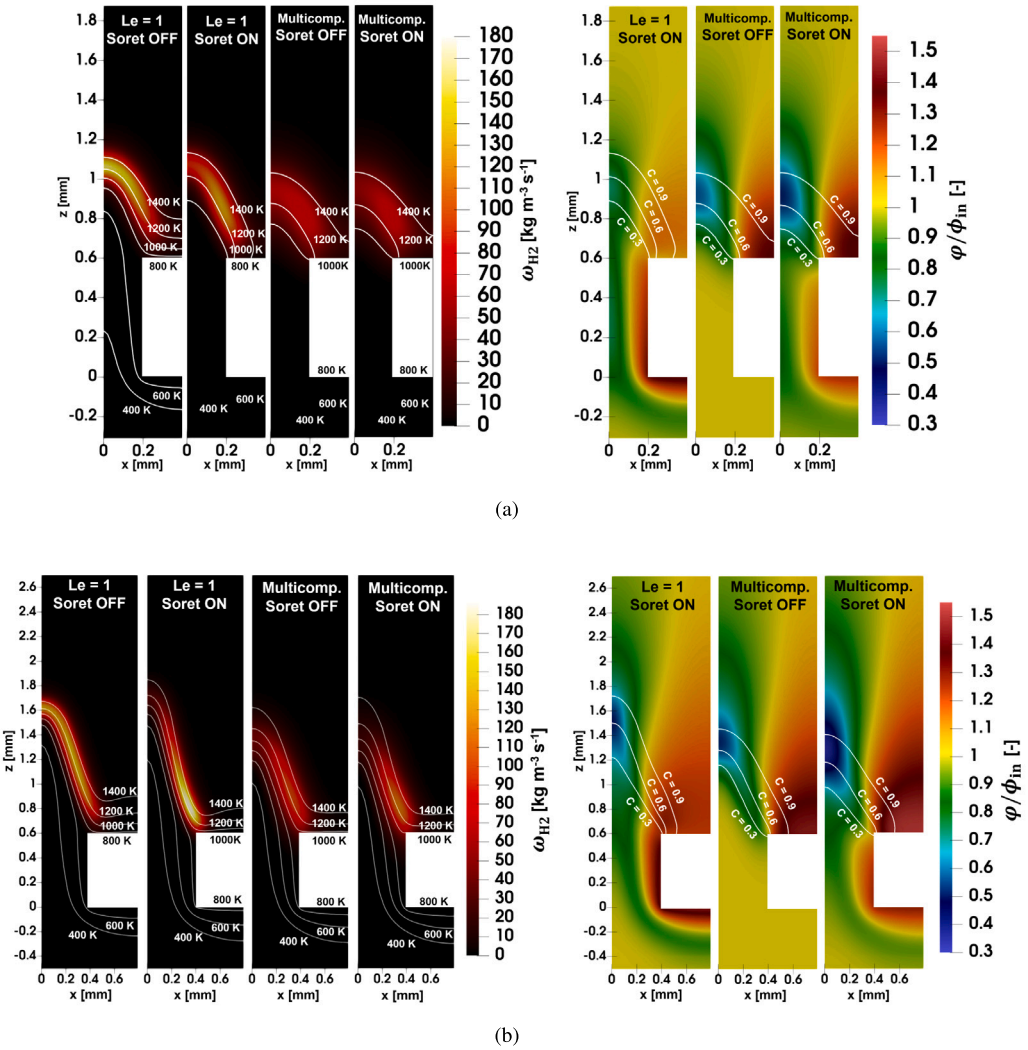

Fig. 5. Visualization of the H_2 consumption rate and normalized local equivalence ratio profiles for the four investigated cases. The hole diameters are $W = 0.4$ mm (a) and $W = 0.8$ mm (b), and the inlet velocity corresponds to $V_S = 4.00$ m/s for all cases. Temperature and progress variable iso-contours are plotted in white.

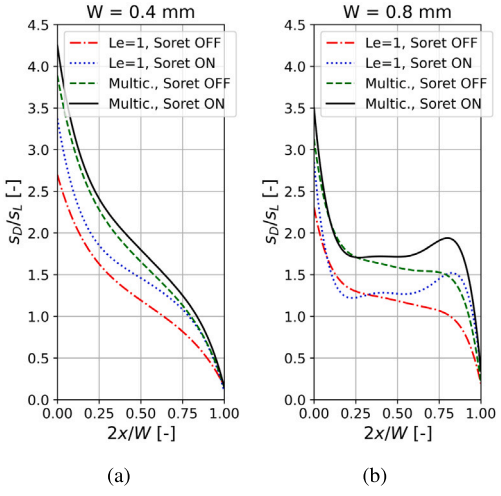

Fig. 6. Normalized displacement speed as a function of the non-dimensional transversal coordinate $2x/W$ for the four investigated cases. The hole diameters are $W = 0.4$ mm (a) and $W = 0.8$ mm (b).

from the center to the wall. Moreover, in the downstream part of the hole, the Soret effect has already pushed most of the fuel toward the wall so that no more fuel remains and the fuel flux toward the wall ceases. For these reasons, no significant variations in the shape of the displacement speed curve are observed in Fig. 6(a) compared to the case without the Soret effect. Moreover, only minor increases in heat flux to the burner plate and in solid temperature are observed as listed in Table 1. In contrast, for larger holes, more fuel is available in the hole and the impact of Soret diffusion is much more pronounced. Due to higher temperature gradients from the center to the wall and greater availability of fuel, significant enrichment is observed in the flame base region for $W = 0.8$ mm. The peak value of ω_{H_2} shifts toward the flame base region, and its maximum value increases. A higher burning intensity near the burner plate raises the solid temperature and the heat flux, further increasing the temperature gradients from the channel center to the wall. This amplifies the Soret effect, which leads to even richer mixtures and higher temperatures close to the wall resulting in a non-linear self-accelerating mechanism. The flame speed is then increased in the critical region close to the wall, as demonstrated by the local maximum observed near the wall in Fig. 6(b), ultimately leading to higher flashback velocities. This mechanism overtakes the dominance of preheating effects for $W = 0.6$ mm, where we observe the blue curve starting to grow in Fig. 4. Note that the impact of preheating is not eliminated in this and the following cases, as doing so

would require eliminating the heat transfer between the gases and the burner plate, which would completely alter the flow and combustion characteristics.

When the multicomponent model is enabled, no significant enrichment at the flame base due to preferential diffusion is observed for $W = 0.4$ mm. The small channel dimension and the high preheating lead to a quasi-hemispherical flame with a reduced absolute value of the curvature, suppressing curvature-induced preferential diffusion effects. The primary impact of the non-unity Lewis number is the thickening of the flame. The impact of preferential diffusion on the laminar flame thickness and speed, as well as fuel consumption rate, is a result of the complex interactions of molecular and thermal transport and the reaction kinetics [23]. Depending on the conditions, preferential diffusion can increase or decrease the flame speed and thickness as well as the consumption rate. Under the investigated lean conditions, diffusion of intermediate species toward both the unburnt and burnt regions spreads the flame front, increasing its thickness and reducing the maximum consumption rate. The augmented thickness increases the contact area between the flame and the burner plate, resulting in higher heat flux and higher burner plate temperatures. As a result, an enhanced preheating of the unburnt mixture is observed, which leads to higher values of s_D and consequently to higher flashback velocities. This mechanism applies to both small and large diameters, as shown in Table 1, where T_B and $\dot{q}$ exhibit comparable increases for both $W = 0.4$ mm and $W = 0.8$ mm when multicomponent diffusion is enabled. For $W = 0.8$ mm, we additionally observe the H_2 consumption at the tip of the flame being 45% of that in the flame base region, due to curvature effects: the larger diameter promotes a conical shape for the flame, facilitating curvature-induced enrichment of the flame base. In conclusion, the enhanced preheating caused by the thickening of the flame leads to increased flashback velocities for both small and large holes, shifting the green curve upward compared to the red one in Fig. 4. Furthermore, preferential diffusion effects become significant for $W > 0.6$ mm, contributing to an increased slope of the curve.

When considering the combined effects of Lewis number and Soret diffusion, we observe the superposition of the previously discussed phenomena. Our detailed analysis of each effect confirms that, in contrast to infinitely long slit configurations, the dependence of the flashback velocity on the size of the circular hole is determined by the relative importance of preheating, the Soret effect, and preferential diffusion. Specifically, the effects of preheating lead to a negative dependence of V_{FB} on W: for small diameters, the heat transfer from the hot burner plate to the fresh gases is more effective, leading to higher flashback velocity compared to larger diameters. In contrast, as W increases, the Soret effect and preferential diffusion tend to increase V_{FB}. Larger holes result in higher temperature gradients from the center to the wall and greater fuel availability, leading to enhanced enrichment of the flame base due to the Soret effect. Moreover, a larger diameter encourages a conical flame shape, facilitating curvature-induced enrichment at the flame base. A greater impact of preferential diffusion effects for larger diameters is consistent with the higher slope of the curve observed in Fig. 2 for leaner mixtures, where preferential diffusion effects are more pronounced. Notably, the combined effect of these two mechanisms leads to a non-trivial optimum for circular holes, corresponding to a minimum of V_{FB} for $W = 0.5$ mm. Additionally, the impact of Soret diffusion is found to play a crucial role, similar to non-unity Lewis numbers, demonstrating that including such effects cannot be neglected for estimations of flashback limits in domestic burners.

4.2. Slits

The investigation is extended to slits with a fixed length of $L = 2$ mm and varying widths within the range $W \in [0.4\text{ mm}–0.8\text{ mm}]$. Flashback velocities are computed across three equivalence ratios, $\phi = 0.6$, 0.8, and 1.0, as shown in Fig. 7. For slits, V_{FB} exhibits a linear dependence on W across the entire investigated range. While the flashback

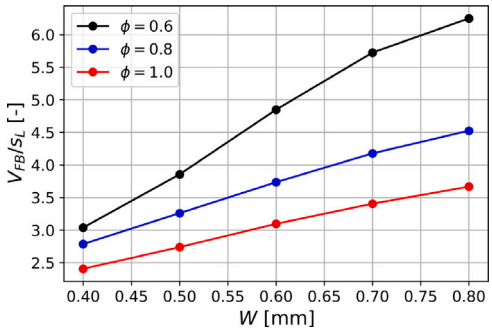

Fig. 7. Normalized flashback velocity as a function of slit width for $\phi = 0.6$, 0.8, and 1.0. (For interpretation of the references to color in this figure legend, the reader is referred to the web version of this article.)

velocity is almost identical to the circular hole case for small widths, its dependence on the slit width is more pronounced, with V_{FB} exceeding that of circular holes by approximately 50% at $W = 0.8$ mm. Notably, unlike the circular hole case, no optimal slit width to prevent flashback is observed. Compared to circular holes, the results suggest a reduced influence of preheating effects and an increased impact of preferential diffusion effects on the relationship between V_{FB} and W for slits. Again, this is consistent with a higher flashback propensity and a more pronounced dependence on the slit width lower equivalence ratios. To better visualize the flashback mechanism in slits, contours of temperature, normalized H_2 consumption rate, and normalized local equivalence ratio on the longitudinal section of the slit are shown in Fig. 8 for the case $W = 0.5$ mm. Due to the elongated shape, the preheating of the fresh gases is only observed at the rounded ends of the slit, where the enclosed geometry promotes heat transfer. As a result, the overall bulk velocity and the flame shape is less influenced by preheating effects compared to circular holes, as these effects are localized only at the slit ends. In the same critical regions, significant enrichment is observed due to both preferential diffusion and the Soret effect for all values of W, leading to the initiation of flashback. Consequently, preferential diffusion and the Soret effect dominate the trend, leading to an almost linear dependence of V_{FB} on W. In general, the flashback mechanisms in slits are similar to those described in Section 4.1 for circular holes, and a more detailed analysis is not deemed necessary: the key differences between circular holes and slits are linked to the reduced impact of the preheating mechanism and the loss of one symmetry in the flow, which leads to the enrichment of the slit extremities resulting in lower resistance to flashback, as they happen preferentially in the curved end-regions of the slits. Hence, the analysis of the individual effects of non-unity Lewis numbers and Soret diffusion is deemed unnecessary here, as it leads to the same conclusions already presented, and can be found in the Supplementary Material.

5. Conclusions

Detailed numerical simulations of lean hydrogen flames in 3D configurations have been conducted to examine the competing effects of preheating, preferential diffusion, and the Soret effect on the dependence of the flashback propensity on the size of holes/slits within perforated burners. The dependence of the flashback velocity on the hole/slit size is found to be driven by the relative importance of these two mechanisms when varying the diameter/width W. Further, we find that both non-unity Lewis numbers and Soret diffusion equally contribute to the increase of the flashback limit and the dependence of the flashback velocity on the size of the hole. Notably, the Soret effect is found to have a leading-order effect on the flashback velocity for larger holes: the enrichment of the region close to the hot walls causes

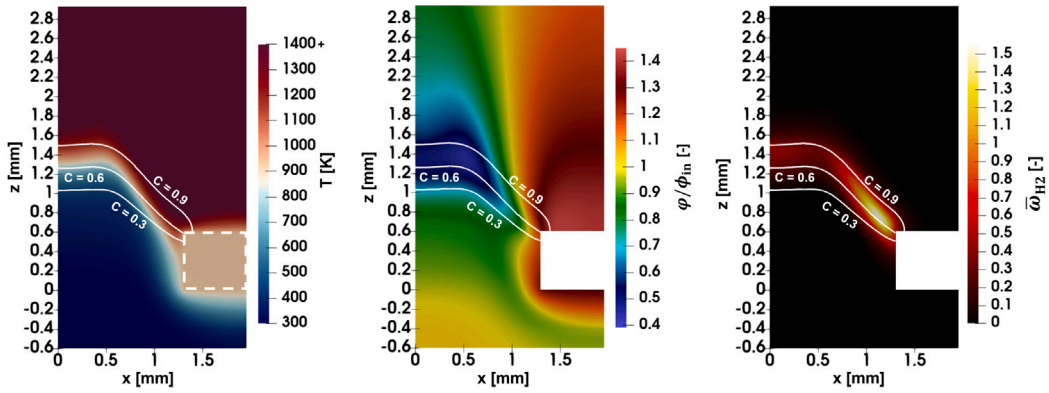

Fig. 8. Visualization of temperature (a), normalized local equivalence ratio (b), and normalized H_2 consumption rate profiles (c) at the flashback limit on the longitudinal section (xz-plane) of the slit for the case $\phi = 0.6$. Progress variable iso-contours are plotted in white. The solid part, corresponding to the slit extremity, is represented by a dashed line.

the flame to burn more intensely at the flame base, further increasing the plate temperature and the temperature gradients that promote the Soret effect, thereby resulting in a non-linear, self-accelerating feedback mechanism. This finding highlights the necessity of including both the Soret effect and the conjugate heat transfer between the fluid and the solid zones in numerical simulations for the estimation of flashback velocities.

For circular holes, a non-monotonic dependence of the flashback velocity on the diameter is observed. Due to the enclosed geometry, the preheating mechanism is dominant for small diameters, while preferential diffusion effects are suppressed, causing V_{FB} to decrease when increasing W. Indeed, preferential diffusion is found to become the dominant mechanism for $W > 0.5$ mm, where the flashback velocity exhibits a strong positive dependence on the hole diameter. An optimum diameter for avoiding flashback is found at $W = 0.5$ mm, where the two mechanisms balance.

In the case of slits, the elongated shape leads to a lower impact of the preheating mechanism and a higher impact of preferential diffusion effects in the investigated range of widths. As only preferential diffusion drives the flashback dependence on the slit width, this relation is linear, and a higher flashback propensity than that of circular holes is observed within the entire investigated range.

Novelty and significance statement

This study pioneers an exploration into three competing mechanisms, namely, preheating of the fresh gases, preferential diffusion, and Soret effect, which determine the dependence of the flashback propensity of lean hydrogen flames within domestic perforated burners on the size of the holes/slits. Due to their enclosed geometry, which promotes heat transfer and higher importance of preheating, circular holes are found to exhibit non-monotonic dependence on hole size, with a non-trivial optimum diameter to avoid flashback. This behavior is specific to circular holes and differs from that observed in previously studied infinitely long slits. These phenomena are further detailed through a novel analysis of the relative impact of non-unity Lewis numbers and Soret diffusion. The Soret effect, in combination with conjugate heat transfer, is found to have a leading-order impact on the flashback limits due to a non-linear self-accelerating feedback mechanism.

CRediT authorship contribution statement

Filippo Fruzza: Conceptualization, Methodology, Data analysis, Writing. **Hongchao Chu:** Reviewing and editing. **Rachele Lamioni:** Conceptualization, Methodology, Reviewing and editing. **Temistocle Grenga:** Reviewing and editing. **Chiara Galletti:** Conceptualization, Reviewing and editing. **Heinz Pitsch:** Conceptualization, Reviewing and editing.

Declaration of competing interest

The authors declare that they have no known competing financial interests or personal relationships that could have appeared to influence the work reported in this paper.

Acknowledgments

This research is partially funded by the Ministry of University and Research (MUR) and Immergas S.p.A., Brescello, RE (Italy), as part of the PON 2014–2020 “Research and Innovation” resources - Green/Innovation Action - DM MUR 1061/2021 and DM MUR 1062/2021.

Appendix A. Supplementary data

Supplementary material related to this article can be found online at https://doi.org/10.1016/j.proci.2024.105581.

References

[1] R. McKenna, Q. Bchini, J. Weinand, J. Michaelis, S. König, W. Köppel, W. Fichtner, The future role of Power-to-Gas in the energy transition: Regional and local techno-economic analyses in Baden-Württemberg, Appl. Energy 212 (2018) 386–400.
[2] W. Liang, Z. Chen, F. Yang, H. Zhang, Effects of soret diffusion on the laminar flame speed and Markstein length of syngas/air mixtures, Proc. Combust. Inst. 34 (1) (2013) 695–702.
[3] H. de Vries, A.V. Mokhov, H.B. Levinsky, The impact of natural gas/hydrogen mixtures on the performance of end-use equipment: Interchangeability analysis for domestic appliances, Appl. Energy 208 (2017) 1007–1019.
[4] A. Aniello, T. Poinsot, L. Selle, T. Schuller, Hydrogen substitution of natural-gas in premixed burners and implications for blow-off and flashback limits, Int. J. Hydrog. Energy (2022).
[5] H. Pers, A. Aniello, F. Morisseau, T. Schuller, Autoignition-induced flashback in hydrogen-enriched laminar premixed burners, Int. J. Hydrog. Energy (2022).
[6] T.B. Kıymaz, E. Böncü, D. Güleryüz, M. Karaca, B. Yılmaz, C. Allouis, İ. Gökalp, Numerical investigations on flashback dynamics of premixed methane-hydrogen-air laminar flames, Int. J. Hydrog. Energy 47 (59) (2022) 25022–25033.
[7] F. Vance, L. de Goey, J. van Oijen, Development of a flashback correlation for burner-stabilized hydrogen-air premixed flames, Combust. Flame 243 (2022) 112045.
[8] F. Vance, L. de Goey, J. van Oijen, Prediction of flashback limits for laminar premixed hydrogen-air flames using flamelet generated manifolds, Int. J. Hydrog. Energy 48 (69) (2023) 27001–27012.
[9] F. Fruzza, R. Lamioni, L. Tognotti, C. Galletti, Flashback of H_2-enriched premixed flames in perforated burners: Numerical prediction of critical velocity, Int. J. Hydrog. Energy 48 (81) (2023) 31790–31801.
[10] E. Flores-Montoya, A. Aniello, T. Schuller, L. Selle, Predicting flashback limits in H_2 enriched CH_4/air and C_3H_8/air laminar flames, Combust. Flame 258 (2023) 113055.

[11] F. Fruzza, R. Lamioni, A. Mariotti, M.V. Salvetti, C. Galletti, Flashback propensity due to hydrogen blending in natural gas: sensitivity to operating and geometrical parameters, Fuel 362 (2024) 130838.
[12] F. Vance, Y. Shoshin, J. van Oijen, L. de Goey, Effect of lewis number on premixed laminar lean-limit flames stabilized on a bluff body, Proc. Combust. Inst. 37 (2) (2019) 1663–1672.
[13] F.H. Vance, P. de Goey, J.A. van Oijen, The effect of thermal diffusion on stabilization of premixed flames, Combust. Flame 216 (2020) 45–57.
[14] F. Fruzza, H. Chu, R. Lamioni, T. Grenga, C. Galletti, H. Pitsch, Preprint: Effects of three-dimensional slit geometry on flashback of premixed hydrogen flames in perforated burners, 2023, http://dx.doi.org/10.48550/arXiv.2312.00744.
[15] R. Bilger, S. Stårner, R. Kee, On reduced mechanisms for methane-air combustion in non-premixed flames, Combust. Flame 80 (2) (1990) 135–149.
[16] Ansys Fluent 22.1 User's Guide, Ansys Inc, 2022.
[17] W.E. Stewart, Multicomponent mass transfer., AIChE J. 41 (1) (1995) 202–203.
[18] H.J. Merk, The macroscopic equations for simultaneous heat and mass transfer in isotropic, continuous and closed systems, Appl. Sci. Res. Sec. A 8 (1) (1959) 73–99.
[19] K. Kuo, R. Acharya, Applications of Turbulent and Multiphase Combustion, EngineeringPro collection, Wiley, 2012.
[20] M. Modest, Radiative Heat Transfer, Elsevier Science, 2013.
[21] K. Kuo, Principles of Combustion, Wiley, 2005.
[22] C. Law, Dynamics of stretched flames, Symp. Combust. Proc. 22 (1) (1989) 1381–1402.
[23] P.E. Lapenna, L.K.W. Berger, F. Creta, H. Pitsch, Hydrogen laminar flames, in: Hydrogen for Future Thermal Engines / Edited By Efstathios-Al. Tingas, in: Green Energy and Technology, Springer International Publishing, Cham, 2023, pp. 93–139.